Synthesis and Characterization of Novel *para*- and *meta*-Phenylenevinylene Derivatives: Fine Tuning of the Electronic and Optical Properties of Conjugated Materials

L. Pascal,[†] J. J. Vanden Eynde,[†] Y. Van Haverbeke,*[,†] P. Dubois,*[,‡] A. Michel,[§] U. Rant,[||] E. Zojer,*[,||] G. Leising,*[,⊥] L. O. Van Dorn,[#] N. E. Gruhn,[#] J. Cornil,[#,▽] and J. L. Brédas*[,#,▽]

Département de Chimie Organique, Université de Mons-Hainaut, Place du Parc 20, B-7000 Mons, Belgium, Service des Matériaux Polymères et Composites, Université de Mons-Hainaut, Place du Parc 20, B-7000 Mons, Belgium, Département de Chimie Biologique, Université de Mons-Hainaut, Place du Parc 20, B-7000 Mons, Belgium, Institut für Festkörperphysik, Technische Universität Graz, Petergasse 16, A-8010 Graz, Austria, Science and Technology, AT&S AG, Fabriksgasse 13, A-8700 Leoben, Austria, Department of Chemistry, The University of Arizona, 1306 East University Boulevard, Tucson, Arizona 85721-0041, and Service de Chimie des Matériaux Nouveaux, Université de Mons-Hainaut, Place du Parc 20, B-7000 Mons, Belgium

Received: March 11, 2002; In Final Form: April 30, 2002

We report the synthesis of novel phenylenevinylene derivatives that allow for the introduction of meta versus para connections on the phenylene rings, as well as the incorporation of nitrogen atoms within the conjugated backbone and the attachment of electroactive substituents. We assess the impact of the various derivatization schemes on the electronic and optical properties by means of gas-phase ultraviolet photoelectron spectroscopy (UPS) and optical absorption and emission measurements; the evolution of the experimental data is further supported by the results of quantum-chemical calculations. We demonstrate that the electronic and optical properties of phenylenevinylene chains, and by extension those of many conjugated materials, can be tuned over a large energy range by a tailored design of the molecular structures.

1. Introduction

Organic conjugated materials are now in the stage of commercialization under the form of active elements in light-emitting diodes (LED) used as pixels in low-resolution matrix displays. A typical LED device is made by sandwiching organic thin film(s) between two metal electrodes.[1,2] The luminescence signal is generated as a result of several processes:[2] (i) injection of electrons and holes in the organic layer from the cathode and the anode, respectively, (ii) migration of the charges in opposite directions under the influence of a static electric field, (iii) recombination of the electrons and holes under the form of intramolecular singlet and triplet excitons, and (iv) radiative decay of the excitons to the ground state. The achievement of high electroluminescence quantum yield requires a balanced injection of the electrons and holes into the organic layer. This is generally fulfilled by the design of multilayer devices in which the emission layer is surrounded by a hole-transporting layer or an electron-transporting layer or both;[3,4] the main role of the hole[electron]-transporting layer is to minimize the barrier between the energy of the highest occupied level [the lowest unoccupied level] of the material and the Fermi energy of the metal at the electrode to ease the injection process. Moreover, the use of several layers can help in creating energy barriers within the organic medium to confine the charge carriers at molecular interfaces and hence generate a preferential zone for the radiative recombination of the electron−hole pairs.[5] Other strategies to balance the electron and hole injection and to improve device performance consist of (i) attaching electron-transport moieties on the conjugated polymer backbones[6,7] or at the end of flexible side chains to avoid changes in the color of emitted light (as is typically observed upon direct attachment of substituents on the backbone[8]), and (ii) blending polymers with electron-transport and hole-transport units.[9,10]

Conjugated materials also emerge as attractive candidates for the fabrication of photodiodes[11−13] and, by extension, solar cells and optical scanners.[14] Such devices generally involve a binary mixture of two chemically distinct conjugated systems, one with a low ionization potential playing the role of the donor and the other with a high electron affinity acting as the acceptor. The conversion of the incident light into an electrical current requires (i) light absorption by the donor or the acceptor or both, (ii) migration of the excitons toward the interface between the two materials (this step can be avoided in homogeneous blends), (iii) exciton dissociation at the molecular interface into charge carriers, for instance, by transferring the electron to the acceptor while keeping the hole on the donor if the latter is initially photoexcited (the efficiency of this photoinduced charge transfer process critically depends on the relative energies of the frontier levels of two materials in interaction),[15] and (iv) charge transport to the electrodes.

These descriptions underscore that the design of efficient LEDs and photodiodes requires a proper energy alignment of the frontier electronic levels of the materials used in the active layers and, hence, strategies to tailor the electronic structure of conjugated materials. It is also of interest to develop routes to

* To whom correspondence should be addressed.
[†] Département de Chimie Organique, Université de Mons-Hainaut.
[‡] Service des Matériaux Polymères et Composites, Université de Mons-Hainaut.
[§] Département de Chimie Biologique, Université de Mons-Hainaut.
[||] Technische Universität Graz.
[⊥] AT&S AG.
[#] The University of Arizona.
[▽] Service de Chimie des Matériaux Nouveaux, Université de Mons-Hainaut.

10.1021/jp025748d CCC: $22.00
Published on Web 06/04/2002

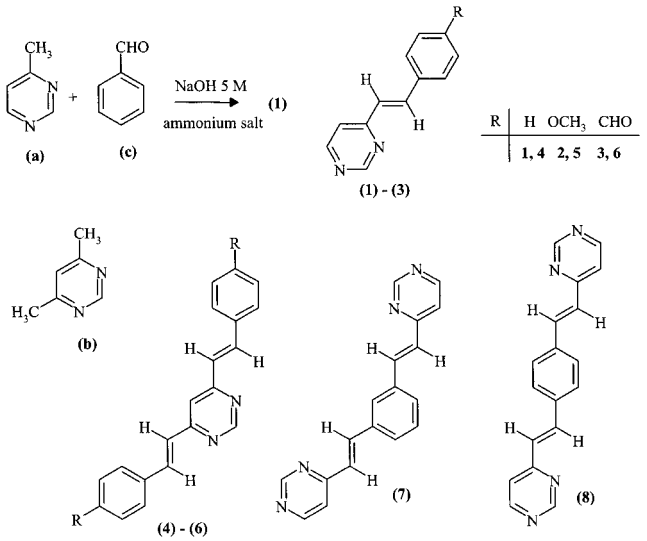

Figure 1. Sketch of the synthetic route and chemical structures of compounds **1**−**8**.

fine-tune the energies of the lowest singlet and triplet excited states of such materials, which are primarily governed by their one-electron structure. This is needed, for instance, to modulate the color of the light emitted by electroluminescent diodes or the efficiency of the energy-transfer processes exploited in electrophosphorescent devices.[16,17] Up to now, the search for the best matching partners in a given application has been achieved in many cases by empirical trials from a wide set of available compounds. This task would be significantly facilitated if the impact of various derivatization schemes could be quantified and exploited to vary, in a controlled way and over a large range, the energies of the frontier one-electron levels and those of the excited states.

We have recently demonstrated that (di)methyldiazines readily react with aromatic aldehydes, in a hot aqueous solution of sodium hydroxide 5 M and in the presence of a catalytic amount (10%) of a quaternary ammonium salt, to afford the expected condensation compounds.[18] In this contribution, we apply this efficient protocol to synthesize novel oligophenylenevinylene derivatives, the chemical structures of which are shown in Figure 1. The focus on conjugated structures derived from oligo(para-phenylenevinylene)s is motivated by the tremendous interest devoted to the parent polymer (PPV) and its substituted derivatives for applications in optoelectronic devices.[3,10,12,15,19,20] The compounds synthesized here are obtained in short reaction times (less than 1 h) and excellent yields (over 70%). In addition, the electronic and optical properties can be modulated by (i) varying the number of repeating units, (ii) controlling the para versus meta connections on the aromatic rings, (iii) varying the number of nitrogen atoms involved along the conjugated path, or (iv) attaching electroactive substituents on the rings. These compounds thus offer a unique opportunity to study on a quantitative basis the impact of the various derivatization schemes on the electronic and optical properties of the chains, which we assess by means of gas-phase ultraviolet photoelectron spectroscopy (UPS) and optical absorption and emission measurements. We demonstrate that cooperation between various effects can lead to significant fluctuations in the energies of the one-electron levels and excited states and can be exploited for a fine-tuning of these properties. The experimental data are further supported by the results of semiempirical quantum-chemical calculations; the very good agreement observed between theory and experiment also validates the use of our quantum-chemical approach as a predictive tool for designing molecules prior to chemical synthesis.

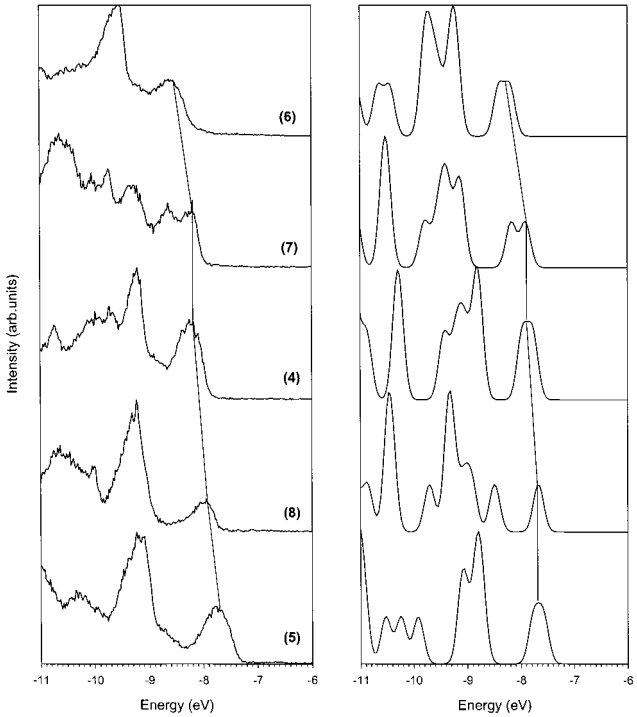

Figure 2. Gas-phase UPS spectra of compounds **5**−**8** (left). The spectra are shown in the order of decreasing HOMO binding energy from top to bottom; corresponding simulations of the UPS spectra at the INDO level are shown in the right panel.

2. Geometric and Electronic Properties

The chemical structures of the molecular compounds under study are illustrated in Figure 1. The most stable conformers are characterized by the following: (i) the coplanarity of the vinylene linkages and the pyrimidine rings; it can be noted that a 180° rotation of the pyrimidine units leads to a less-stable structure due to the activation of steric effects between adjacent hydrogen atoms; (ii) a torsion angle on the order of 15°−25° between the plane of the vinylene units and that of the adjacent benzene rings as a result of steric interactions between hydrogen atoms; (iii) a full conjugation between the π-atomic orbitals in the methoxy and aldehyde groups and those of the aromatic rings to which they are attached, as already shown by previous calculations for methoxy substituents.[21]

On the basis of these structural data, we investigate the way in which the energy of the HOMO level is affected by the various derivatization schemes. To do so, we report in Figure 2 the gas-phase UPS spectra of the three-ring oligomers together with the corresponding intermediate neglect of differential overlap (INDO) simulations; we also collect in Table 1 the energy of the HOMO and LUMO levels calculated at the INDO level for all of the compounds. The experimental results show that the energy of the HOMO level spans a range of ∼0.8 eV among the three-ring compounds.

We first focus on the way in which the meta connections impact the electronic structure of the oligomers. Comparison between the experimental and theoretical UPS spectra allows us to assign the peak around −7.9 eV in **8** to the optical signature of the HOMO level and the doublet observed at higher binding energy in **7** to the HOMO and HOMO-1 levels. The influence of the meta versus para connection is illustrated by the change in the HOMO level energy when going from **8** to **7**;

TABLE 1: Experimental and Theoretical Energies of the HOMO Level of Compounds 1−8 as Estimated from Gas-Phase UPS Spectra and INDO Calculations, Respectively, and the Energy of the LUMO Level Calculated at the INDO Level

	HOMO/INDO[a] (eV)	HOMO/UPS[a] (eV)	LUMO/INDO (eV)
1	−7.98		−0.54
2	−7.74		−0.52
3	−8.27		−1.07
4	−7.77 (−8.02)	−8.11 (−8.33)	−0.65
5	−7.58 (−7.82)	−7.61 (−7.85)	−0.63
6	−8.18 (−8.46)	−8.42 (−8.70)	−1.24
7	−7.90	−8.19	−0.68
8	−7.67	−7.93	−0.90

[a] Values in parentheses are the energy of the HOMO-1 level when the UPS peak with the lowest binding energy corresponds to the superposition of two electronic levels.

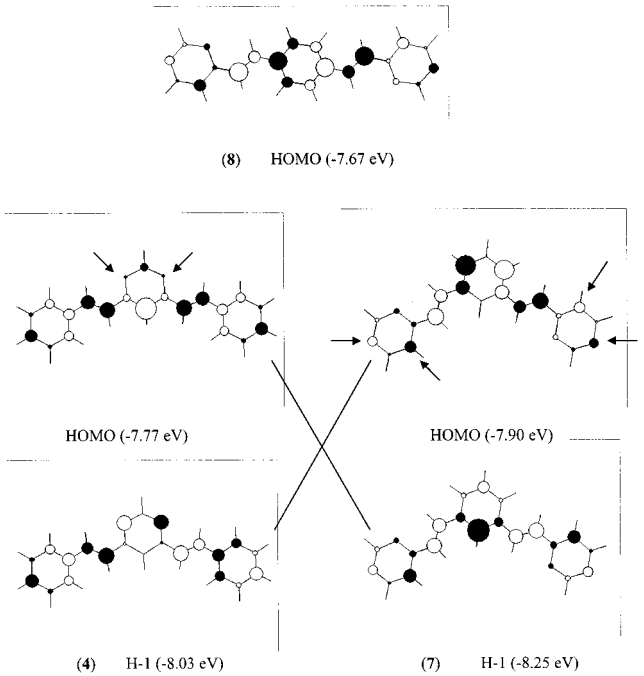

Figure 3. LCAO pattern of the highest occupied levels in compounds **4**, **7**, and **8** (assumed to be in a planar conformation). The size and color of the circles over the atoms correspond to the amplitude and sign of the LCAO coefficient associated with the π atomic orbitals. The arrows denote the location of the nitrogen atoms in compounds **4** and **7**.

the UPS data show a significant stabilization of the HOMO level by 0.26 eV upon introduction of the meta connection, which is fully reproduced by the INDO calculations. In contrast, the calculations indicate that the LUMO level is destabilized by ∼0.2 eV. This leads to a total increase in the HOMO−LUMO difference by some 0.46 eV when going from **8** to **7**; note that similar results are calculated between the corresponding hydrocarbon derivatives. This evolution is rationalized by the linear combination of atomic orbitals (LCAO) patterns of the HOMO and LUMO levels in the two compounds showing a break of conjugation in the central ring when the meta connection is introduced (as illustrated for the HOMO level in Figure 3). The reduction in the degree of delocalization by meta bridging has also been demonstrated by previous AM1 calculations performed on *m*-phenylenevinylene oligomers containing from two to seven rings; these results pointed to the very slow evolution of the HOMO and LUMO energy with chain size.[22] The rupture of conjugation induced by meta connections has been largely exploited in the design of high-spin radical cations as a preliminary step toward organic magnets.[23] Note also that the theoretical estimates of the HOMO energy are underestimated by ∼0.3 eV with respect to the experimental values. This contrasts with a similar joint study performed on the 4,4′-bis-(*N*-*m*-tolyl-*N*-phenylamino)biphenyl (TPD) molecule and substituted derivatives in which a remarkable quantitative agreement was found between the INDO calculations and the gas-phase UPS data.[24] On the basis of previous calculations performed in gas phase, we attribute the present discrepancy to the slight changes in the total energy of PPV-like oligomers when modulating the torsion angles between the vinylene units and the aromatic rings up to ∼40°; this may lead to actual torsion angles larger than those obtained at the AM1 level[21] (and hence to larger values of the HOMO energy).

We now turn to the role played by the nitrogen atoms in determining the energy of the frontier electronic levels in the various compounds. The introduction of four nitrogen atoms to yield compounds **7** and **8** induces at the INDO level a stabilization on the order of 0.4−0.5 eV for both the HOMO and LUMO levels with respect to the corresponding hydrocarbon derivatives; this trend is in agreement with the results obtained in a previous theoretical study based on INDO calculations.[25] However, the stabilization of the HOMO and LUMO levels does not exclusively correlate with the number of nitrogen atoms in the molecule and is actually also very sensitive to their positions along the molecular backbone. Although no general trends prevail, the changes in the one-electron structure between two compounds differing only by the position and number of nitrogen atoms along the conjugated backbone can be rationalized by the results of our quantum-chemical calculations. This is demonstrated in Figure 2; the evolution of the intense peak observed around −8.0 eV in the UPS spectrum of **4** (which corresponds to the superposition of the highest two occupied levels) into a doublet in **7** is well-reproduced by the theoretical simulations. The doublet in **7** is made of two individual peaks separated by 0.45 eV in the UPS spectrum, while a value of 0.35 eV is obtained at the INDO level. The theoretical results further indicate that the HOMO level of **4** has an equivalent level stabilized by ∼0.5 eV in **7** in which it corresponds to the H-1 level, see Figure 3. This evolution is rationalized by the fact that the nitrogen atoms in **4** are located on sites possessing a very small electronic density on the HOMO level, in contrast to the situation found for the equivalent level in **7**. For similar reasons, the H-1 level of **4** is destabilized by 0.13 eV in **7** in which it becomes the highest occupied level. Globally, the calculations thus show that the HOMO level is stabilized by 0.13 eV when going from **4** to **7**, while the UPS spectrum provides an estimate on the order of 0.07 eV.

Next, we address the influence of electroactive substituents attached on the conjugated backbone by comparing the UPS spectra of **4**, **5**, and **6**. The INDO simulations indicate for the three compounds that the lowest binding energy peak corresponds to the overlapping signature of the HOMO and HOMO-1 levels. A peak fitting of the experimental line shapes can however provide the energy of the individual levels; this procedure yields energy separations between the highest two occupied levels that are in full agreement with the INDO calculations (see Table 1). The UPS data and the calculations show that the attachment of formyl groups on the terminal carbon atoms of **4** to give **6** leads to a significant stabilization of the HOMO level by 0.3 and 0.4 eV, respectively. The influence of substituents is governed by the interplay between the inductive effects taking place in the σ skeleton and the mesomer effects associated with the π electrons. The stabiliza-

tion of the HOMO level upon formyl substitution results from their σ-acceptor and π-acceptor characters, which both depopulate the electronic density over the molecular backbone and hence stabilize the frontier electronic levels. The INDO calculations yield a stabilization of the LUMO level by 0.6 eV when attaching the aldehyde groups; the asymmetry in the stabilization of the HOMO and LUMO levels will have strong implications on the optical properties of the oligomers, as discussed in the next section. In contrast, both the experimental and theoretical results indicate that the introduction of methoxy groups leads to a destabilization of the HOMO level; this confirms that the effects linked to the π-donor character of the methoxy groups dominate over those associated with their σ-acceptor character. Similarly, the LUMO level is slightly destabilized upon methoxy substitution as a result of the counteracting influence of the inductive and mesomer effects. The HOMO shift estimated at the INDO level is underestimated with respect to the experimental value (0.2 versus 0.5 eV); this discrepancy cannot be attributed to the INDO parametrization, which has been shown to provide results comparing remarkably well to gas-phase UPS spectra in the case of the TPD molecule and methoxy-substituted derivatives.[24] We attribute this discrepancy once again to the underestimation of the actual torsion angles in the gas-phase conformations; the good quantitative agreement observed between the experimental and theoretical HOMO energy for **5** suggests that the conformation of this molecule is less twisted than that in the other compounds and is actually very close to that calculated at the AM1 level. We stress that the electronic properties could be further tuned by varying the nature, number, and position of the substituents over the conjugated backbone.[26] Very similar trends are calculated for the two-ring compounds when going from the unsubstituted backbone **1** to the derivatives substituted by a methoxy **2** and an aldehyde **3** group; the HOMO energy in these compounds is, however, systematically stabilized with respect to the values obtained for the corresponding three-ring oligomers because of the shortening of the conjugated backbone.

All together, our joint theoretical and experimental characterization demonstrates that the HOMO and LUMO energies of oligo(phenylenevinylene) chains can be deeply modulated by exploiting various derivatization schemes, which can act cooperatively. We can formulate general guidelines as follows, starting from a paraphenylenevinylene oligomer of a given size as a reference compound: (i) the HOMO level is stabilized by shortening the chain size, introducing nitrogen atoms, inserting meta-linkages, and attaching substituents with a π-acceptor or σ-acceptor character; it gets destabilized by increasing the chain length and substituting the backbone with groups having a π-donor or σ-donor character; (ii) the LUMO is stabilized by the increase in chain length, the introduction of nitrogen atoms, and the attachment of substituents with a π-acceptor or σ-acceptor character; this level is destabilized by the reduction of chain length, the incorporation of meta-connections, and the attachment of groups with a π-donor or σ-donor character.

The very good agreement observed between the experimental data and the theoretical calculations suggests that a molecular design aimed at matching a specific electronic property can be first accomplished at the theoretical level prior to chemical synthesis. In particular, the results show that the electron affinity of a three-ring *meta*-phenylenevinylene oligomer can be increased by 1.0 eV following the introduction of nitrogen atoms in the phenylene rings and the attachment of aldehyde groups (with π-acceptor and σ-acceptor characters). This is of great interest for application in (opto)electronic devices in which compounds with a high electron affinity are required in order to (i) allow for the injection of electrons in organic layers from environmentally stable metallic electrodes, characterized by high work functions, (ii) promote exciton dissociation in molecular blends used in photodiodes, or (iii) ensure efficient electron transport not hampered by trapping associated with oxygen contamination.[27,28]

TABLE 2: Experimental and Theoretical Transition Energies of the Lowest Optical Transition and Associated Molar Extinction Coefficient (ϵ_{max}, in L/mol cm) of Compounds 1−8[a]

	INDO/SCI		dichloromethane		ethanol	
	energy (eV)	ϵ_{max}	energy (eV)	ϵ_{max}	energy (eV)	ϵ_{max}
1	4.09	28 500	3.96	28 500	3.92	28 500
2	3.96	31 000	3.67	28 500	3.63	28 500
3	3.96	36 000	3.81	40 000	3.80	36 000
4	3.76	34 000	3.59	36 500	3.59	34 500
5	3.67	38 500	3.45	36 000	3.36	36 500
6	3.66	46 500	3.51	50 000	3.49	50 000
7	4.02	52 500	3.94	53 000	3.89	52 500
8	3.62	52 000	3.44	51 000	3.42	53 000

[a] The calculated molar extinction coefficients have been scaled with respect to the experimental value obtained for compound **1**.

3. Optical Properties

The lowest transition energy of oligo(paraphenylenevinylene)s decreases nearly linearly as a function of the inverse number of monomer units along the chains, as evidenced by experimental[29,30] and calculated[31] absorption and photoluminescence spectra. As a result of this chain-length evolution, short oligomers emit in the blue while longer chains are characterized by a yellow-green emission;[31] the energy of the lowest optical transition can thus be varied by up to 1 eV when modulating the chain length, with the steepest evolution being observed among the short chains. It is thus of interest to explore the way in which the absorption and emission properties are affected for short chains by the incorporation of para versus meta connections as well as by the introduction of nitrogen atoms or electroactive substituents or both along the backbone; to do so, we analyze below the absorption and emission spectra of compounds **1**−**8**.

The optical absorption spectra of compounds **1**−**8** have been recorded in dilute solutions ($C = 2 \times 10^{-5}$ M) of ethanol and dichloromethane at room temperature. These two solvents have been chosen to investigate the influence of solvent polarity (dielectric constants of 9.08 and 24.30 for dichloromethane and ethanol, respectively) on the absorption spectra. We collect in Table 2 the experimental transition energy and molar extinction coefficient of the lowest absorption band in the eight compounds. The spectra are found to be very similar in the two solvents, except for a slight red shift of the transition energies when going from dichloromethane to ethanol, thus with increasing solvent polarity. We also report in Table 2 the transition energies calculated at the INDO/SCI level for the oligomers, assumed in first approximation to be in a planar conformation, together with the relative intensities of the lowest absorption band scaled with respect to the experimental value obtained for compound **1**. Despite a very good agreement between the experimental and simulated spectra, we observe that the calculated transition energies are slightly overestimated with respect to the experimental values. Because calculations performed on twisted backbones would increase the energy difference between the theoretical and experimental values, we attribute most of this shift to the neglect of the solvent effects in our calculations; the latter are expected to stabilize the energy

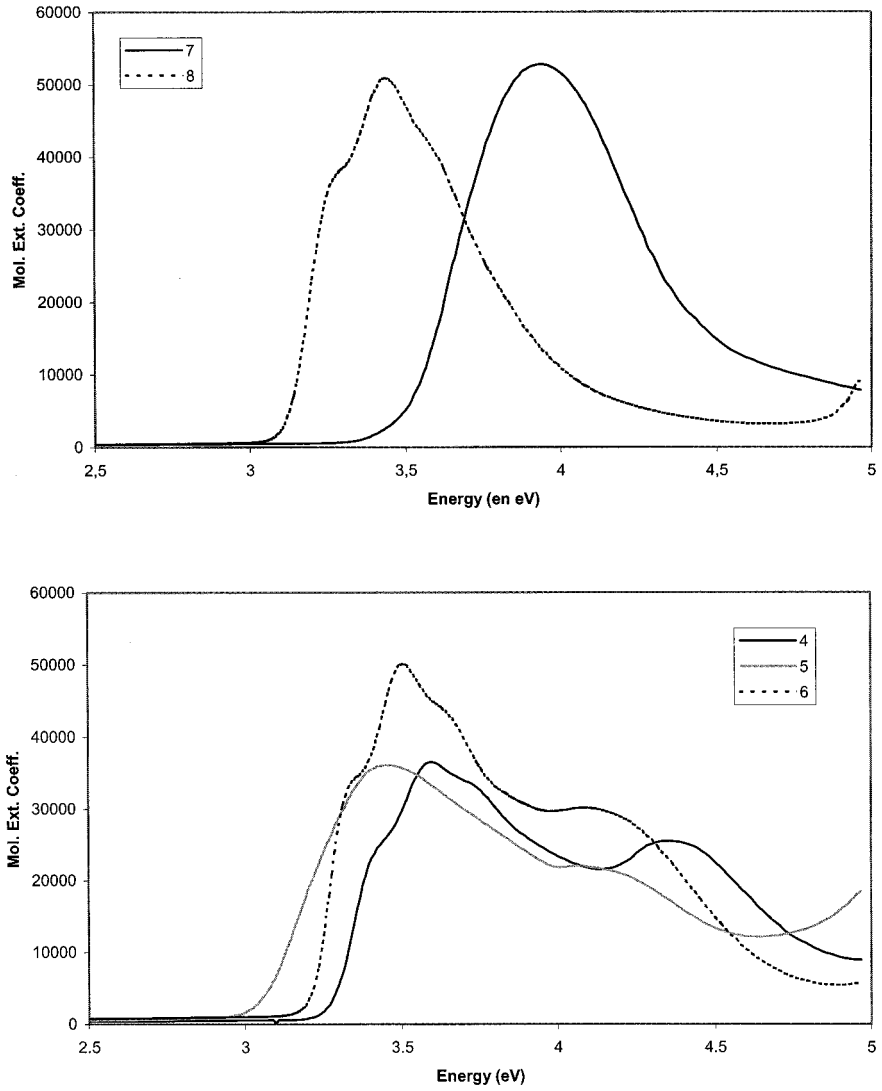

Figure 4. Optical absorption spectra of compounds **7** and **8** (top) and compounds **4**, **5**, and **6** (bottom) in dichloromethane.

of the lowest excited state because of the partial charge-transfer taking place in all of the compounds from the phenylene to the pyrimidine rings.

We display in Figure 4 the absorption spectra of compounds **7** and **8** obtained in dichloromethane. The lowest absorption band has a similar intensity for the two compounds; however, the transition energy of the oligomer with para connections on the central ring is red shifted by 0.5 eV with respect to the oligomer displaying meta connections, in full agreement with the quantum-chemical calculations. The lowest absorption band of **8** originates from the lowest excited state of the oligomer, which is primarily described by an electronic excitation from HOMO to LUMO; in contrast, the calculations show that the lowest absorption band of **7** results from the superposition of three distinct excited states. These results demonstrate that the introduction of meta connections prevents an efficient delocalization of the electronic wave function over the conjugated backbone and, hence, a significant red shift of the lowest optical transition with chain length; this is supported by experimental data[32,33] and previous calculations on oligo(metaphenylene-vinylene)s showing a vanishingly small bathochromic shift of the lowest optical transition in chains containing up to five monomer units.[22]

The energy and intensity of the lowest optical transition of compound **8** are very similar to those computed for the corresponding hydrocarbon backbone (i.e., the three-ring PPV oligomer). This is driven by the fact that both transitions are primarily described by a HOMO−LUMO excitation and that the incorporation of nitrogen atoms leads to an almost symmetric stabilization of the HOMO and LUMO levels (0.53 and 0.45 eV, respectively). Thus, in para-connected chains, we can conclude that the nitrogen atoms strongly impact the one-electron structure of the chains but only slightly affect the energy of the lowest absorption and emission bands. The situation is much more complex in derivatives in which the lowest optical absorption band does not originate from a single excited state mostly described by a HOMO−LUMO excitation, as is the case for the oligomers incorporating meta connections. The calculations indicate that compound **7** and the corresponding hydrocarbon chain are both characterized by a single absorption band centered around 4.0 eV, resulting from the superposition of three distinct excited states; in contrast, they predict for compound **4** that this band is split into two features around 3.7 and 4.5 eV with an approximate 10/6 intensity ratio, which is fully consistent with the experimental absorption spectra.

We have also investigated the impact of the electroactive substituents on the optical properties of the oligomers. Figure 4 also illustrates the way in which the absorption of compound **4** is modified when attaching methoxy or formyl groups on the terminal carbon atoms. In both cases, a slight red shift of the

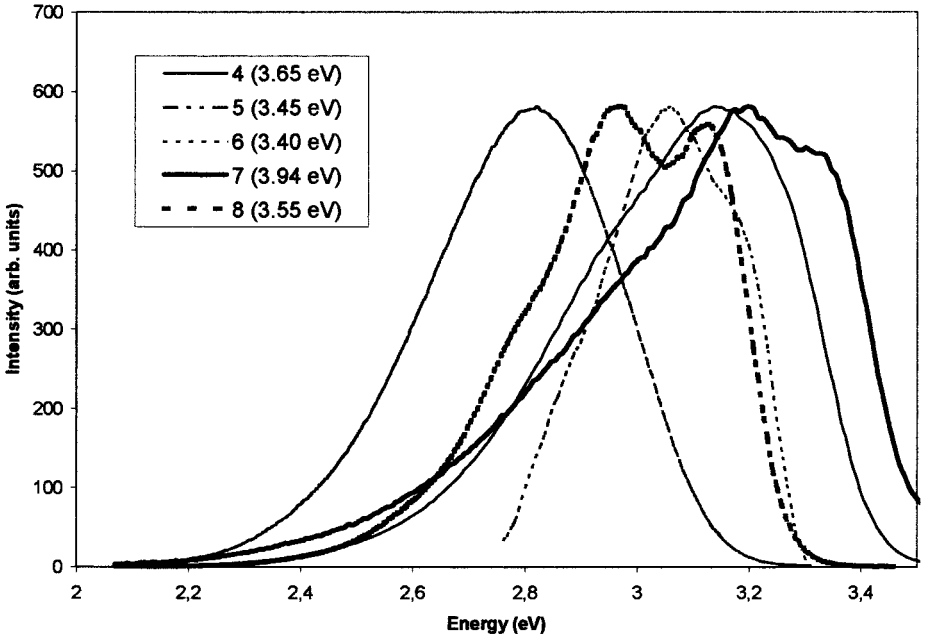

Figure 5. Emission spectra of compounds **4**−**8** measured in dichloromethane. We report in parentheses the excitation energy used for each compound; the spectra have been normalized with respect to the emission of compound **4**.

lowest optical transition is observed upon substitution. Because the lowest absorption feature of **4** observed around 3.6 eV is mainly described by a HOMO−LUMO excitation, the red shift is rationalized by the fact that the methoxy [formyl] groups lead to an asymmetric destabilization [stabilization] of the frontier electronic levels, which reduces the electronic band gap, as discussed in the previous section. These trends are supported by experimental and theoretical data reported on oligo(para-phenylenevinylene)s substituted by cyano or methoxy groups or both.[26] A similar evolution is also observed for the two-ring compounds when going from **1** to the substituted derivatives **2** and **3**; their lowest optical transition is, however, blue-shifted and reduced in intensity with respect to the three-ring oligomers as a result of the chain shortening.

In summary, the theoretical and experimental data demonstrate that meta connections prevent a progressive red shift of the lowest optical transition in phenylenevinylene oligomers of increasing length; this is of particular interest in the search for new attractive candidates to be used as blue emitters in optoelectronic devices. The energy of the lowest optical transition can be further fine-tuned by attaching electroactive substituents or incorporating nitrogen atoms along the conjugated backbone or both. The results also show that nitrogen atoms can be used in some cases to strongly modify the one-electron properties of conjugated chains (i.e., the ionization potential and electron affinity) without affecting their absorption and emission properties. We emphasize that the energy of the lowest absorption band can also be modulated by the protonation of the nitrogen atoms involved in the conjugated path,[34] as described in previous experimental studies;[35] a detailed description of such effects is beyond the scope of the present paper and will be discussed elsewhere.

We report in Figure 5 the emission spectra of the three-ring compounds recorded in dichloromethane and collect in Table 3 the measured λ_{max} values; we also report in Table 3 the λ_{max} values obtained in ethanol, as well as the corresponding fluorescence quantum yields. Except for compound **8**, the emission spectra are structureless, thus pointing to a pronounced conformational disorder of the emitting chains in solution. As is the case for the absorption spectra, the λ_{max} of the emission spectra are weakly affected by the solvent (a small red shift is observed when going from dichloromethane to ethanol). The close match observed between the absorption and excitation spectra for all of the compounds confirms that the photogenerated electron−hole pairs decay into the lowest excited state before giving rise to light emission. Table 3 indicates that the energy difference between the transition energy at the maximum of the absorption and emission bands varies significantly among the compounds. This reflects the amplitude of the geometry relaxation taking place in the lowest excited state upon photoexcitation and is expected to decrease with conjugation length;[30] this is consistent with the marked increase in this energy difference when going from compounds **8** to **7** (i.e., when breaking conjugation by the introduction of meta connections). Because of these variations in the amplitude of the geometry relaxation effects, the evolution of the transition energy of the emission band among the various compounds does not fully parallel that observed for the lowest absorption band; this points to the fact that geometry relaxation effects have to be taken into account at the theoretical level to provide accurate locations of the energy of the lowest excited state in its equilibrium geometry.

TABLE 3: Experimental Transition Energies (in eV) of the Emission Band of Compounds 4−8 in Dichloromethane and Ethanol and Corresponding Shift Defined as the Energy Difference between the Maximum of the Absorption and Emission Bands and the Fluorescence Quantum Yield (Φ_F) Measured in Ethanol

	dichloromethane		ethanol		
	energy (eV)	shift	energy (eV)	shift	Φ_F
4	3.12	0.47	3.01	0.58	0.034
5	2.82	0.63	2.64	0.72	0.076
6	3.05	0.46	2.79	0.72	0.010
7	3.20	0.74	3.08	0.81	0.012
8	3.11	0.33	2.97	0.45	0.034

The fluorescence quantum yields in compounds **4**−**8** are rather low (systematically below 10%) when compared to those in oligo(*para*-phenylenevinylene)s, typically characterized by values between 50% and 90%;[29] values above 50% have also been reported for phenylenevinylene backbones incorporating

both meta and para connections.[37] In contrast, the efficiency of light emission of the stilbene molecule in solution is generally much lower as a result of a trans−cis photoisomerization mechanism[38] (note that no fluorescence signal is detected for the two-ring oligomers, **1**−**3**). Recent experimental studies have also indicated that the fluorescence quantum yield is strongly reduced for PPV oligomers displaying torsions along the backbone upon substitution.[38] The low quantum efficiency of the three-ring compounds under study thus points to the existence of a mechanism competing with the radiative decay route in the lowest excited state. This quenching can be associated with the following: (i) an intersystem crossing process (ISC) from the singlet to the triplet manifold induced by torsions along the conjugated backbone[38,39] and leading to the population of the lowest triplet excited state (and possibly to a weak phosphorescence signal at longer time scales[40]); the broadness of the emission bands is consistent with the presence of torsions along the backbone, which are required for the ISC process to occur in conjugated backbones without heavy atoms; or (ii) a photoinduced twisted intramolecular charge transfer (TICT) process leading to a complete separation between the electron and hole as a result of a twist of the central part of the chain; this mechanism has been identified in aminostilbazonium ions.[41]

These torsions responsible for reducing the fluorescence quantum yield are likely to be induced by a subtle interplay between the presence of nitrogen atoms along the backbone and solvation effects. This is supported by the change in fluorescence quantum yield observed for the most emissive compound **5** when going from ethanol to dicholoromethane (from 0.076 to 0.041, respectively). It is worth stressing that the solid-state packing will tend to planarize the chains in the absence of significant steric effects and, hence, to strongly reduce the efficiency of the ISC process; similarly, the possible formation of the highly twisted excited states involved in the TICT process should be strongly hindered in the solid state.

4. Conclusions and Perspectives

In this work, we have shown that the electronic and optical properties of a class of conjugated compounds can be widely modulated through molecular engineering. This has been illustrated by comparing the properties of novel phenylene-vinylene derivatives, in which chain legnth, incorporation of nitrogen atoms, attachment of electroactive substituents, and introduction of meta versus para connections can be controlled through our synthetic approach.

We have assessed on a quantitative basis the impact of the various derivatization schemes on the electronic and optical properties of the chains by means of gas-phase UPS, optical absorption, and fluorescence measurements. The evolution of the properties among the derivatives has been further rationalized by the results of quantum-chemical calculations, which can thus provide useful guidelines for molecular engineering. We stress that the present results are applicable to many other conjugated oligomeric backbones.

Acknowledgment. The work in Mons is partly supported by the Belgian Federal Governement (PAI 4/11), the European Community for general support in the frame of "Objectif 1: Materia Nova", and the Belgian National Fund for Scientific Research (FNRS/FRFC). The work at Arizona is partly supported by National Science Foundation (Grant CHEM-0078819), the Office of Naval Research, the IBM Shared University Research Program, the Petroleum Research Fund, and the Department of Energy. The gas-phase UPS were measured at the Center for Gas-Phase Electron Spectroscopy at The University of Arizona. J.C. is an FNRS research associate; L.P. acknowledges a grant from the Fonds pour la Formation à la Recherche dans l'Industrie et dans l'Agriculture (FRIA).

Appendix: Experimental and Theoretical Section

Synthesis. 4-Methyl- (a) or 4,6-dimethylpyrimidine (b) reacts with benzaldehyde (c) in a hot aqueous solution of sodium hydroxide (5 M) and in the absence of any organic solvent to yield compounds **1**−**8** (see Figure 1).[18] The reactions do not occur without a catalyst; the addition of a quaternary ammonium salt (such as Aliquat 336 or tetrabutylammonium hydrogen sulfate; 10 mol %) substantially favors the kinetics of formation of the expected condensation compounds; the latter are obtained in short reaction times (less than 1 h) and excellent yields (more than 70%). Interestingly, the crude products can be isolated by a mere filtration thus limiting the use of an organic solvent for purification by recrystallization (except for compounds **3** and **6**, see below). Solvents and reagents are commercially available (Acros Organics, Aldrich Co) and were used without further purification. Melting points (uncorrected) were determined on a Electrothermal 9100 apparatus. NMR spectra ($CDCl_3$) were recorded on a JEOL JNP-PMX 60 spectrometer (60 MHz for ^1H at 1.4 T) or a Bruker AMX spectrometer (300 MHz for ^1H and 75 MHz for ^{13}C at 7.0 T). Chemical shifts are given in ppm using TMS as internal reference. IR spectra were recorded on a Perkin-Elmer FTIR 1760K spectrophotometer. The elemental analyses were carried out at the Departement de Chimie Pharmaceutique of the Université de Liège (Belgium). High-resolution mass spectra have been recorded on a Micromass Auto Spec 6F, resolving power ca. 10 000 (5% valley), electron ionization, 70 eV energy, 200 μA trap current, PFK reference compound. Compounds (yield) **1** (90%),[42] **2** (90%),[43] **3** (80%),[44] **4** (90%),[45] and **5** (90%)[46] have already been described in the literature.

*General Procedure for the Preparation of Compounds **1**, **2**, **4**, **5**, and **7**.* A stoichiometric mixture of the (di)methylpyrimidine and the aromatic aldehyde in an aqueous solution (25 mL for 5 mmol of the heterocycle) of sodium hydroxide (5 M) containing Aliquat 336 or tetrabutylammonium hydrogen sulfate (10 mol % vs the heterocycle) was heated under reflux for 1 h. After cooling, the crude product was filtered off and recrystallized.

*Preparation of Compound **3**.* A stoichiometric mixture of 4-methylpyrimidine and benzene-1,4-dicarboxaldehyde mono-(diethyl acetal) in an aqueous solution (25 mL for 5 mmol of the heterocycle) of sodium hydroxide (5 M) containing Aliquat 336 or tetrabutylammonium hydrogen sulfate (10 mol % versus the heterocycle) was heated under reflux for 1 h. After cooling, the reaction mixture was extracted with dichloromethane (75 mL). The solution was dried on magnesium sulfate, and the solvent was removed by evaporation under reduced pressure. The residue, 4-{2-[4-(diethoxymethyl)phenyl]ethenyl}pyrimidine, was dissolved in acetone (50 mL), and a small amount (0.5 mL) of concentrated hydrochloric acid was added under agitation. Compound **3** precipited in the acetone and has been filtered off and recrystallized.

*Preparation of Compound **6**.* The procedure used to obtain compound **3** was applied to 4,6-dimethylpyrimidine.

*Preparation of Compound **8**.* A stoichiometric mixture of 4-methylpyrimidine and 4-[2-(4-pyrimidyl)ethenyl]benzaldehyde **3** in an aqueous solution (25 mL for 5 mmol of the heterocycle) of sodium hydroxide (5 M) containing Aliquat 336 or tetra-

butylammonium hydrogen sulfate (10 mol % vs the heterocycle) was heated under reflux for 1 h. After cooling, the crude product was filtered off and recrystallized.

4-[2-(4-Pyrimidinyl)ethenyl]-4′-[2-(6-pyrimidinyl)ethenyl]-benzaldehyde (6). Yield: 85%. M.p. (CH_3CN) 230 °C (decomposition). ^{1}H NMR δ 10.0 (2H, s), 9.1 (1H, s), 8.0 (2H, d, 16 Hz), 7.9 (4H, d, 8 Hz), 7.7 (4H, d, 10 Hz), 7.3 (1H, s), 7.2 (2H, d, 16 Hz) ppm. ^{13}C NMR not available (solubility too low). IR (KBr) 1696, 1602, 1576, 810, 515 cm^{-1}. Anal. Calcd. for $C_{22}H_{16}N_2O_2$: C, 77.63; H, 4.74; N, 8.23. Found: C, 76.88; H, 4.86; N, 8.21. HRMS Calcd. for $C_{22}H_{16}N_2O_2$: 340.121 178. Found: 340.121 140.

4,4′-(1,3-Phenylenedi-2,1-ethenediyl)bis-pyrimidine (7). Yield: 70%. M.p. (CH_3CN) 182−4 °C. ^{1}H NMR δ 9.2 (2H, s), 8.6 (2H, d, 6 Hz), 7.9 (2H, d, 16 Hz), 7.8 (1H, s), 7.6−7.1 (5H, m), 7.0 (2H, d, 16 Hz). ^{13}C NMR δ 161.9, 158.9, 157.5, 136.7, 136.2, 129.4, 128.3, 126.8, 126.2, 118.8 ppm. IR (KBr) 1636, 1572, 1461, 1386, 988 cm^{-1}. Anal. Calcd. for $C_{18}H_{14}N_4$: C, 75.50; H, 4.93; N, 19.57. Found: C, 75.40; H, 4.97; N, 19.58. HRMS Calcd. for $C_{18}H_{14}N_4$: 286.121 847. Found: 286.122 187.

4,4′-(1,4-Phenylenedi-2,1-ethenediyl)bis-pyrimidine (8). Yield: 90%. M.p. (DMSO) 234−6 °C. ^{1}H NMR δ 9.2 (2H, s), 8.7 (2H, d, 6 Hz), 7.9 (2H, d, 16 Hz), 7.6 (4H, s), 7.3 (2H, d, 6 Hz), 7.1 (2H, d, 16 Hz) ppm. ^{13}C NMR δ 161.9, 158.9, 157.5, 136.7, 136.6, 128.3, 128.2, 126.3, 118.9 ppm. IR (KBr) 1634, 1568, 1385, 847, 564 cm^{-1}. Anal. Calcd. for $C_{18}H_{14}N_4$: C, 75.50; H, 4.93; N, 19.57. Found: C, 75.55; H, 4.87; N, 19.64. HRMS Calcd. for $C_{18}H_{14}N_4$: 286.121 847. Found: 286.121 283.

Experimental Characterization. The HeI gas-phase photoelectron spectra of five different oligophenylenevinylenes were recorded using an instrument that features a 36-cm radius, 8-cm gap hemispherical analyzer (McPherson) and custom-designed excitation source, sample cells, and detection and control electronics that have been described in more detail previously.[47] The oligophenylenevinylenes sublimed cleanly with no evidence of decomposition products in the gas phase or as a solid residue. The samples sublimed between 120 and 220 °C (10^{-4} Torr); **4** sublimed at 120−140 °C, **5** at 170−190 °C, **6** at 200−220 °C, **7** at 150−160 °C, and **8** at 160−180 °C. These temperatures were monitored using a "K"-type thermocouple passed through a vacuum feedthrough and attached directly to the sample cell. The argon $^2P_{3/2}$ ionization at 15.759 eV was used as an internal calibration lock of the absolute ionization energy. The difference between the argon $^2P_{3/2}$ ionization and the methyl iodide $^2E_{1/2}$ ionization at 9.538 eV was used to calibrate the ionization energy scale. During data collection, the instrument resolution (measured using fwhm of the argon $^2P_{3/2}$ peak) was 0.020−0.035 eV. All data are intensity-corrected with an experimentally determined instrument analyzer sensitivity function. The HeI spectrum was also corrected for HeIβ resonance line emission from the source, which is about 3% the intensity of the HeIα line emission and at 1.869 eV higher photon energy. The first two ionization peaks were fit using two asymmetric Gaussian peaks.[48] Ionization peak potentials are reproducible to $\pm$0.02 eV ($\sim 3\sigma$ level).

The optical absorption spectra were recorded with a Varian Cary 50 spectrophotometer in ethanol or in dichloromethane ($C = 2 \times 10^{-5}$ M). Excitation and emission spectra were measured on a Shimadzu RF5301PC fluorimeter in dichloromethane ($C = 5$ μg/mL). Fluorescence quantum yields, Φ_f, were determined on a Perkin-Elmer MPF-2A fluorimeter from the integrated fluorescence spectra of dilute solutions (absorbance at the excitation wavelength, 350 nm, being lower than 0.1) in ethanol; 7-amino-4-methylcoumarin, with a reported quantum yield of 0.75 in ethanol,[49] was taken as the reference compound. We stress that the PPV-like oligomer and the reference compound all emit in a wavelength range at which the spectral sensitivity of the fluorimeter is almost constant.

Theoretical Characterization. The geometries of all of the molecular compounds were optimized with the help of the semiempirical Hartree−Fock AM1 (Austin Model 1) Hamiltonian, which has been parametrized to accurately reproduce ground-state geometric structures.[50] All of the internal degrees of freedom are optimized to provide the structural data used as input in the simulation of the gas-phase UPS spectra. On the basis of the optimized geometries, we have calculated the one-electron structure of the compounds by means of the spectroscopic version of the semiempirical intermediate neglect of differential overlap (INDO) Hamiltonian developed by Zerner and co-workers.[51] The UPS spectra are simulated at the INDO level within Koopmans' approximation, as described in refs 52 and 53, in which the choice of our approach to describe the nature of the highest occupied levels of organic conjugated materials was validated. The optical absorption spectra are computed by coupling the INDO Hamiltonian to a single configuration interaction (SCI) scheme; all of the π levels of the molecules are involved in the generation of the singly excited configurations to ensure size consistency. Our previous studies have demonstrated that this technique is successful in describing the nature and the energies of the lowest excited states of organic conjugated molecules.[54,55]

References and Notes

(1) Sheats, J. R.; Antoniadis, H.; Hueschen, M.; Leonard, W.; Miller, J.; Moon, R.; Roitman, D.; Stocking, A. *Science* **1996**, *273*, 884.

(2) Friend, R. H.; Gymer, R. W.; Holmes, A. B.; Burroughes, J. H.; Marks, R. N.; Taliani, C.; Bradley, D. D. C.; dos Santos, D. A.; Brédas, J. L.; Lögdlund, M.; Salaneck, W. R. *Nature* **1999**, *397*, 121.

(3) Tang, C. W.; van Slyke, S. A. *Appl. Phys. Lett.* **1987**, *51*, 913.

(4) Pardo, D. A.; Jabbour, G. E.; Peyghambarian, N. *Adv. Mater.* **2000**, *12*, 1249.

(5) Greenham, N. C.; Moratti, S. C.; Bradley, D. D. C.; Friend, R. H.; Holmes, A. B. *Nature* **1993**, *365*, 268.

(6) Chung, S. J.; Kwon, K. Y.; Lee, S. W.; Jin, J. I.; Lee, C. H.; Lee, C. E.; Park, Y. *Adv. Mater.* **1998**, *10*, 1112.

(7) Zheng, M.; Ding, L. M.; Gurel, E. E.; Lahti, P. M., Karasz, F. E. *Macromolecules* **2001**, *34*, 4124.

(8) Lee, Y.; Chen, X.; Chen, S. A.; Wei, P. K.; Fann, W. S. *J. Am. Chem. Soc.* **2001**, *123*, 2296.

(9) Cao, Y.; Parker, I. D.; Yu, G.; Zhang, C.; Heeger, A. J. *Nature* **1999**, *397*, 414.

(10) Ohmori, Y.; Hironaka, Y.; Yoshida, R.; Fujii, A.; Tada, N.; Yoshino, K. *Polym. Adv. Technol.* **1997**, *8*, 403.

(11) Sariciftci, N. S.; Smilowitz, L.; Heeger, A. J.; Wudl, F. *Science* **1992**, *258*, 1474.

(12) Halls, J. J. M.; Walsh, C. A.; Greenham, N. C.; Marseglia, E. A.; Friend, R. H.; Moratti, S. C.; Holmes, A. B. *Nature* **1995**, *376*, 498.

(13) Smolenyak, P.; Peterson, R.; Nebesny, K.; Törker, M.; O'Brien, D. F.; Armstrong, N. R. *J. Am. Chem. Soc.* **1999**, *121*, 8628.

(14) Yu, G.; Wang, J.; McElvain, J.; Heeger, A. J. *Adv. Mater.* **1998**, *17*, 1431.

(15) Halls, J. J. M.; Cornil, J.; dos Santos, D. A.; Silbey, R.; Wang, D. H.; Holmes, A. B.; Brédas, J. L.; Friend, R. H. *Phys. Rev. B* **1999**, *60*, 5721.

(16) Baldo, M. A.; O'Brien, D. F.; You, Y.; Shoustikov, A.; Silbey, S.; Thompson, M. E.; Forrest, S. R. *Nature* **1998**, *395*, 151.

(17) Cleave, V.; Yahioglu, G.; Le Barny, P.; Friend, R. H.; Tessler, N. *Adv. Mater.* **1999**, *11*, 285.

(18) Vanden Eynde, J. J.; Pascal, L.; Dubois P.; Van Haverbeke Y. *Synth. Commun.* **2001**, *31*, 3167.

(19) Kraft, A.; Grimsdale, A. C.; Holmes, A. B. *Angew. Chem., Int. Ed.* **1998**, *37*, 403.

(20) *Primary Photoexcitations in Conjugated Polymers: Molecular Exciton versus Semiconductor Band Model*; Sariciftci, N. S., Ed.; World Scientific: Singapore, 1997.

(21) Lhost, O.; Brédas, J. L. *J. Chem. Phys.* **1992**, *96*, 5279.

(22) Karabunarliev, S.; Baumgarten, M.; Tyutyulkov, N.; Müllen, K. *J. Phys. Chem.* **1994**, *98*, 11892.

(23) Wienk, M. M.; Janssen, R. A. J. *J. Am. Chem. Soc.* **1997**, *119*, 4492.
(24) Cornil, J.; Gruhn, N. E.; dos Santos, D. A.; Malagoli, M.; Lee, P. A.; Barlow, S.; Thayumanavan, S.; Marder, S. R.; Armstrong, N. R.; Brédas, J. L. *J. Phys. Chem. A* **2001**, *105*, 5206.
(25) Cornil, J.; Beljonne, D.; dos Santos, D. A.; Brédas, J. L. *Synth. Met.* **1996**, *76*, 101.
(26) Cornil, J.; dos Santos, D. A.; Beljonne, D.; Brédas, J. L. *J. Phys. Chem.* **1995**, *99*, 5604.
(27) Horowitz, G. *Adv. Mater.* **1998**, *10*, 365.
(28) Katz, H. E.; Lovinger, A. J.; Johnson, J.; Kloc, C.; Siegrist, T.; Li, W.; Lin, Y. Y.; Dodabalapur, A. *Nature* **2000**, *404*, 478.
(29) Peeters, E.; Ramos, A. M.; Meskers, S. C. J.; Janssen, R. A. J. *J. Chem. Phys.* **2000**, *112*, 9445.
(30) Cornil, J.; Beljonne, D.; Heller, C. M.; Campbell, I. H.; Laurich, B. K.; Smith, D. L.; Bradley, D. D. C.; Müllen, K.; Brédas, J. L. *Chem. Phys. Lett.* **1997**, *278*, 139.
(31) Burroughes, J. H.; Bradley, D. D. C.; Brown, A. R.; Marks, R. N.; Friend, R. H.; Burn, P. L.; Holmes, A. B. *Nature* **1990**, *347*, 359.
(32) Lane, P. A.; Cadby, A. J.; Mellor, H.; Martin, S. J.; Lidzey, D. G.; Bradley, D. D. C.; Lipson, S. M.; O'Brien, D. F.; Blau, W. *Phys. Rev. B* **2000**, *62*, 15718.
(33) Liao, L.; Pang, Y.; Ding, L.; Karasz, F. E. *Macromolecules* **2001**, *34*, 7300.
(34) Pascal, L.; Vanden Eynde, J. J.; Van Haverbeke, Y.; Dubois, P.; Cornil, J.; Brédas, J. L. Manuscript in preparation.
(35) Egelhaaf, H. J.; Gierschner, J.; Oelkrug, D. *Synth. Met.* **1996**, *83*, 221.
(36) Wang, H.; Helgeson, R.; Ma, B.; Wudl. F. *J. Org. Chem.* **2000**, *65*, 5862.
(37) Müllner, R.; Winkler, B.; Stelzer, F.; Tasch, S.; Hochfilzer, C.; Leising, G. *Synth. Met.* **1999**, *105*, 129.
(38) Gierschner, J.; Lüer, L.; Oelkrug, D.; Musluoglu, E.; Behnisch, B.; Hanack, M. *Adv. Mater.* **2000**, *12*, 757.
(39) Beljonne, D.; Shuai, Z.; Pourtois, G.; Brédas, J. L. *J. Phys. Chem. A* **2001**, *105*, 3899.
(40) Hertel, D.; Setayesh, S.; Nothofer, H. G.; Scherf, U.; Müllen, K.; Bässler, H. *Adv. Mater.* **2001**, *13*, 65.
(41) Ephardt, H.; Fromherz, P. *J. Phys. Chem.* **1989**, *93*, 7717.
(42) Gabriel, S.; Colman, J. *Chem. Ber.* **1903**, *36*, 3379.
(43) Haroutounian, S.; Katzenellenbogen, J. *Tetrahedron* **1995**, *51*, 1585.
(44) Hasegawa, M.; Endo, Y.; Aoyama, M.; Saigo, K. *Bull. Chem. Soc. Jpn.* **1989**, *62*, 1556.
(45) Strul, M.; Zugravescu, I. *Rev. Roum. Chim.* **1971**, *16*, 1877.
(46) Reynolds, G. A.; Drexhage, K. H. *Opt. Commun.* **1975**, *13*, 222.
(47) Westcott, B. L.; Gruhn, N. E.; Enemark, J. H. *J. Am. Chem. Soc.* **1998**, *120*, 3382 and references therein.
(48) Lichtenberger, D. L.; Copenhaver, A. S. *J. Electron Spectrosc. Relat. Phenom.* **1990**, *50*, 335.
(49) Reynolds, G. A.; Drexhage, K. H. *Opt. Commun.* **1975**, *13*, 222.
(50) Dewar, M. J. S.; Zoebisch, E. G.; Healy, E. F.; Stewart, J. J. P. *J. Am. Chem. Soc.* **1985**, *107*, 3902.
(51) Zerner, M. C.; Loew, G. H.; Kichner, R. F.; Mueller-Westerhoff, U. T. *J. Am. Chem. Soc.* **1980**, *102*, 589.
(52) Cornil, J.; Vanderdonckt, S.; Lazzaroni, R.; dos Santos, D. A.; Thys, G.; Geise, H. J.; Yu, L. M.; Szablewski, M.; Bloor, D.; Lögdlund, M.; Salaneck, W. R.; Gruhn, N. E.; Lichtenberger, D. L.; Lee, P. A.; Armstrong, N. R.; Brédas, J. L. *Chem. Mater.* **1999**, *11*, 2436.
(53) Hill, I. G.; Kahn, A.; Cornil, J.; dos Santos, D. A.; Brédas, J. L. *Chem. Phys. Lett.* **2000**, *317*, 444.
(54) Cornil, J.; dos Santos, D. A.; Crispin, X. A.; Silbey, R.; Brédas, J. L. *J. Am. Chem. Soc.* **1998**, *120*, 1289.
(55) Brédas, J. L.; Cornil, J.; Beljonne, D.; dos Santos, D. A.; Shuai, Z. *Acc. Chem. Res.* **1999**, *32*, 267.